space. Similarly, rocking curves calculated with dynamical theory show the contribution from each of the multiple beams peaked at the 200 node even though F_{200} is explicitly zero in the calculation. This feature of multiple-beam diffraction is also clearly shown by the δ functions present in the perturbation treatment of Shen (1986). The existence of sharp rocking curves does not require a non-zero structure factor, and multiple-beam effects are neither spread out in reciprocal space nor suppressed by a zero F_{200}.

A null F_{200} neither contributes to scattering nor suppresses the scattering from all of the other nodes in reciprocal space, even for nodes far from the Ewald sphere. At a randomly selected φ angle, one should expect measurable multiple-beam effects at the 200- and 420-type nodes in reciprocal space, even if F_{200} and F_{420} are zero. Also at the 622- and 442-type nodes, integrated intensities will, in general, differ from those predicted by the small but non-zero F_{622} and F_{442} (Tischler & Batterman, 1984). In both cases, ignoring the multiple-beam effects from nodes far from the Ewald sphere leads to inaccurate conclusions.

These results seem to explain the basis-forbidden reflection measurements of Post & Ladell (1987) that show a clear effect where the 311 and 002 nodes intersect the Ewald sphere. Just as many other multiple reflections were important at the 200 reflection examined in this work, the 'three-beam' case of 311 and 002 measured by Post & Ladell will also include many multiple-beam contributions. These extra contributions come from pairs of allowed reflections whose indices sum to 002, and must be included to calculate properly the diffracted intensity.

For the 200 measurements presented here, the narrow rocking-curve widths rule out surface diffraction as a possible source of error because surface peaks would be much wider. Harmonic contamination of the rocking curves can also be ruled out because any harmonic diffracting from the 400 reflection would remain constant with φ, whereas both the calculated and the measured integrated intensities approach zero at $\varphi = 0$ for our experimental conditions.

VI. Concluding remarks

We have shown that the 200 structure factor is zero within the experimental accuracy, and that all of the scattering intensity can be understood by performing multiple-beam calculations. Both the theoretical calculations and measurements show that easily measurable sharp rocking curves are to be expected at the 200 reflection and hence explain the observations of Post & Ladell (1987). It is important to note that the 200 integrated intensities are due to multiple-scattering contributions rather than a nonzero F_{200}.

References

CHAPMAN, L. D., YODER, D. R. & COLELLA, R. (1981). *Phys. Rev. Lett.* **46**, 1578-1581.

CROMER, D. T. & MANN, J. B. (1968). *Acta Cryst.* A**24**, 321-324.

DAWSON, B. (1967). *Proc. R. Soc. London Ser. A*, **298**, 255-263.

HENRY, N. F. M. & LONSDALE, K. (1952). *International Tables for X-ray Crystallography*, Vol. I, p. 341. Birmingham: Kynoch Press.

POST, B. & LADELL, J. (1987). *Acta Cryst.* A**43**, 173-179.

SHEN, Q. (1986). *Acta Cyrst.* A**42**, 525-533.

TISCHLER, J. Z. & BATTERMAN, B. W. (1984). *Phys. Rev. B*, **30**, 7060-7066.

TISCHLER, J. Z. & BATTERMAN, B. W. (1986). *Acta Cryst.* A**42**, 510-514.

Acta Cryst. (1988). A**44**, 25-33

On the X-ray Analysis of Thin Subsurface Layers. Bicrystal Diffraction Analogues

BY A. M. AFANAS'EV AND S. S. FANCHENKO

I. V. Kurchatov Institute of Atomic Energy, 123182 *Moscow, USSR*

(*Received* 30 *March* 1987; *accepted* 5 *August* 1987)

Abstract

X-ray determination of strain and damage distributions in thin subsurface layers from rocking curves is an ambiguous procedure. In the case of N distorted layers, all equivalent profiles can be obtained in the kinematical limit and their total number may be sufficiently large, being of the order of magnitude 2^N [Afanas'ev & Fanchenko (1986). *Dokl. Akad. Nauk SSSR*, **287**, 1395-1399]. A more detailed theoretical treatment of the problem and the analytical expressions of all bicrystal-equivalent crystal

0108-7673/88/010025-09$03.00

structures (crystal structures leading to the same diffraction intensity as the crystal with constant spacing deviation in the subsurface layer) are presented.

1. Introduction

X-ray diffraction methods have been widely used for research into crystal surface damage arising from impurity diffusion, ion implantation and other external sources of destruction (Burgeat & Taupin, 1967; Burgeat & Colella, 1969; Bonse, Hart & Schwuttke, 1969; Yogi, Miyamoto & Nishizava, 1970; Awano, Speriosu & Wilts, 1984). Recently these methods have been applied to the investigation of heterostructures, superlattices and epitaxial films (Quillec, Goldstein, Le Roux, Burgeat & Primot, 1984; Halliwell, Lyons & Hill, 1984). The impurity contamination results in lattice-parameter variation and in partial crystal amorphization, usually described by the statistical Debye–Waller factor. Burgeat & Taupin (1967) based their X-ray rocking-curve analysis on the Takagi–Taupin equations (Takagi, 1962; Taupin, 1964) to account for the spacing dependence on the non-homogeneous impurity distribution near the surface in the dynamical model. Diffraction from thin layers is weak and may be described by the simple kinematical model (Afanas'ev, Kovalchuck, Kovev & Kohn, 1977; Kamenou, Hirai, Asama & Sakai, 1979; Speriosu, Glass & Kobayashi, 1979). A kinematical treatment of the diffraction problem allows one to obtain such integral values as the average distorted layer thickness, degree of amorphization and spacing variation (Afanas'ev, Kovalchuck, Kovev & Kohn, 1977), as well as the detailed distorted layer structures, the strain and damage distributions being fitted directly (Speriosu, Glass & Kobayashi, 1979). Recently the ability to investigate distorted crystal structure was enhanced by means of triple-crystal diffractometry (Eisenberger, Alexandropoulos & Platzman, 1972; Afanas'ev, Kovalchuck, Lobanovich, Imamov, Aleksandrov & Melkonyan, 1981; Afanas'ev, Aleksandrov, Imamov, Lomov & Zav'alova, 1984; Afanas'ev, Aleksandrov & Imamov, 1986). Owing to the diffuse scattering separation precise rocking-curve measurements are available at very large angular deviations from the Bragg angles in this scheme. As a result, high spatial resolution may be achieved, and Yakimov, Chaplanov, Afanas'ev, Aleksandrov, Imamov & Lomov (1984) and Afanas'ev, Aleksandrov, Fanchenko, Chaplanov & Yakimov (1986) have investigated distorted layers consisting of several single atomic layers using this method. The angular deviation from the Bragg angle was three orders of magnitude greater than the rocking-curve width in these experiments. Diffraction at such great deviation angles has been called asymptotic Bragg diffraction (Afanas'ev, Aleksandrov & Imamov, 1986). The complete theoretical analysis of the diffraction data of the problem under consideration was carried out by Afanas'ev & Fanchenko (1986) who have suggested a new method of reconstruction of the equivalent crystal structures leading to the same diffraction intensity in the kinematical model. Their method was applied to the diffraction analysis of ion-implanted layers by Zav'alova, Imamov, Lomov, Marguschev & Maslov (1987).

In § 2 the problem of diffraction from a single crystal with a thin subsurface distorted layer will be discussed. In § 3 examples will be presented of dual distorted profiles leading to the same diffraction intensity; in § 4 the general analysis of the equivalent-solution-reconstruction problem will be carried out, and in § 5 analytical expressions are considered for the crystal structures of the diffraction analogues of a crystal with constant interplanar spacing deviation Δd and Debye–Waller factors e^{-W}, *i.e.* a bicrystal. The derivation of these expressions is given in the Appendix.

2. Diffraction from a crystal with a thin subsurface distorted layer

The analysis of the diffraction from a single crystal with a thin subsurface distorted layer will be given in the case of symmetric reflection shown schematically in Fig. 1, the thickness of the distorted layer being L. The reflection from the thin distorted layer is weak and its amplitude M_N can be expressed, in the case of $\Delta\theta \ll \theta_B$, as

$$M_N(\Delta\theta) = BR_N(\Delta\theta)$$
$$= B\sum_{n=1}^{N} \exp\left[i(n-N-1)(\Delta\theta+\theta_1)2\pi\cot\theta_B - W_n + i\varphi_n\right] \quad (1)$$
$$B = i\chi_h\pi/2\sin\theta\sin\theta_B,$$
$$\varphi_n = -2\pi\sum_{k=n+1}^{N+1}\Delta d_{k-1k}/d_0,$$
$$\theta_1 = \chi_0/\sin 2\theta_B,$$

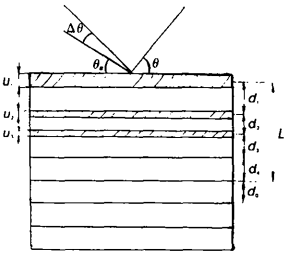

Fig. 1. The symmetric diffraction scheme. The atomic planes are represented by the solid lines, the root-mean-square atom deviations from the atomic planes u_n are represented by the dashed regions, the nth interplanar spacing in the distorted layer is noted as d_n.

where θ is the angle of incidence, θ_B is the Bragg angle, Δd_{n-1n} is the nth interplanar spacing deviation, d_0 is the ideal crystal spacing, $\Delta\theta = \theta - \theta_B$ is the angular deviation from the Bragg angle, N is the number of single atomic planes in the distorted layer, $\exp(-W_n)$ is the nth atomic plane Debye-Waller factor, and χ_0, χ_h are the Fourier components of the elementary cell polarizability. The Debye-Waller factor may be expressed *via* the value of the root-mean-square atomic displacements from the atomic planes u_n as (shown schematically in Fig. 1)

$$\exp(-W_n) = \exp(-8\pi^2 \sin^2\theta_B u_n^2/\lambda^2),$$

with λ representing the X-ray wavelength.

The total diffraction amplitude from the distorted crystal $M(\Delta\theta)$ includes the diffraction amplitudes from the thin distorted layer and from the undistorted crystal as well as the multiple-scattering amplitudes. The total diffraction amplitude $M(\Delta\theta)$ can be expressed as an expansion in the small parameter M_N (M_N is apparently proportional to the value of the ratio L/L_{ext} where L_{ext} is the extinction depth). These expansion coefficients are given *via* the value of the ideal crystal diffraction amplitude $M_0(\Delta\theta)$ defined as

$$M_0(\Delta\theta) = y - (y^2-1)^{1/2}\,\mathrm{sign}\, y,$$
$$y = -(2\Delta\theta \cos\theta_B \sin\theta + \chi_0)/\chi_h.$$

Within the framework of second-order perturbation theory for the intensity, one should take into account the second-order terms in the small parameter M_N in the total-amplitude expansion. The absorption and the imaginary parts of χ_0, χ_h will be neglected in the following analysis for simplicity. One can thus obtain the following expression for the total diffraction amplitude M:

$$M(\Delta\theta) = M_0(\Delta\theta)[1-|M_N(\Delta\theta)|^2] + M_N(\Delta\theta) - M_0^2(\Delta\theta)M_N^*(\Delta\theta) + M_0^3(\Delta\theta)M_N^{*2}(\Delta\theta).$$

This expansion is similar to the corresponding expansion used by Afanas'ev, Kovalchuck, Kovev & Kohn (1977) and is illustrated schematically in Fig. 2. The trivial algebraic transformations and the apparent identities

$$1 + M_0^2 = 2yM_0, \qquad 1 - M_0^2 = 2M_0(y^2-1)^{1/2}\,\mathrm{sign}\, y$$

allow one to express the second-order-perturbation-theory diffraction intensity $I(\Delta\theta)$ in the form

$$I(\Delta\theta) = |M(\Delta\theta)|^2 = \begin{cases} 1 & |y| \le 1 \\ |M_0(\Delta\theta)|^2 \left| 1 + 2\,\mathrm{sign}\, y (y^2-1)^{1/2} M_N(\Delta\theta) - \dfrac{2(y^2-1)^{1/2} M_N^2(\Delta\theta)}{|y| + (y^2-1)^{1/2}} \right|^2 & |y| > 1. \end{cases} \quad (2)$$

One should emphasize that the total reflection region, $|y| \le 1$ or $|\Delta\theta| \le \theta_0$, with θ_0 representing the Darwin table width, is insensitive to the thin distorted layer at least in second-order perturbation theory in the small parameter M_N. Within the linear approximation in M_N one arrives at the following expression for the intensity:

$$I(\Delta\theta) = \begin{cases} 1 & |y| \le 1 \\ I_0(\Delta\theta)[1 + 4\,\mathrm{sign}\, y (y^2-1)^{1/2} \times \mathrm{Re}\, M_N(\Delta\theta)] & |y| > 1, \end{cases} \quad (2^*)$$

where $I_0(\Delta\theta)$ is the ideal crystal diffraction intensity. Since the diffraction intensity from the undistorted crystal is great in the small-angular-deviation region, the second-order corrections in M_N are practically indistinguishable as the background is present; hence one can use (2*) for the intensity in the region of small angular deviations $\Delta\theta \sim \theta_0$ and reconstruct only $\mathrm{Re}\, M_N(0)$ from the diffraction data.

For large deviation angles $|\Delta\theta| \gg \theta_0$, $|y| \gg 1$, the difference between y and $(y^2-1)^{1/2}$ is negligible and expression (2) for the diffraction intensity is equivalent to the corresponding kinematical expression. The total kinematical diffraction amplitude M is expressed as the sum of the diffraction amplitudes M_0 and M_N,

$$M = M_0 + M_N,$$

where M_N is given by (1), the refraction angular shift θ_1 being neglected, and $M_0(\Delta\theta)$ is represented as

$$M_0(\Delta\theta) = B/(1-e^{iq}), \qquad q = 2\pi \cot\theta_B \Delta\theta.$$

The kinematical diffraction intensity is given by

$$I(\Delta\theta) = |M|^2 = I_0(\Delta\theta)|1 + (1-e^{iq})R_N(\Delta\theta)|^2. \quad (3)$$

As in the analysis above the term linear in R_N in (3) is proportional to $\mathrm{Re}\, M_N(\Delta\theta)$ for small $\Delta\theta \to 0$. Consequently, the region of small $\Delta\theta$, where one should use the exact formula (2*), gives practically no new information compared with the kinematical angular region considered in (3). This fact allows one to consider only the asymptotic Bragg diffraction region $\Delta\theta \gg \theta_0$. Another angular restriction, $\Delta\theta \ll \theta_B$, used earlier lets one neglect the Debye-Waller-factor and phase-shift dependences on the relatively small deviation angle $\Delta\theta$.

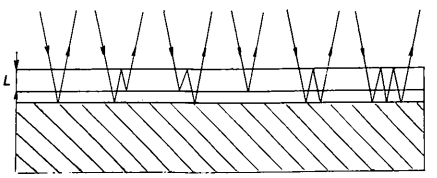

Fig. 2. The multiple-reflecting processes from a crystal with a thin distorted layer; the ideal-crystal region is dashed.

The asymptotic Bragg diffraction angular region

$$\theta_0 \ll \Delta\theta \ll \theta_B \tag{4}$$

justifies itself from the theoretical point of view as well as from the experimental one. In practice the diffraction intensity for $\Delta\theta \sim \theta_B$ is too small to measure and for $\Delta\theta \sim \theta_0$ the diffraction intensity from the undistorted crystal region is too great to distinguish the thin-distorted-layer weak contribution to the total diffraction intensity.

The kinematical model is therefore adequate for the description of diffraction from thin distorted layers, but the reconstruction of the crystal layer scattering characteristics from rocking curves is an ambiguous problem, only the diffraction intensity being measured and the all phase information being lost. This ambiguity is a rather general and well known one, but only recently the ambiguity problem and the problem of reconstructing all equivalent solutions have been solved by Afanas'ev & Fanchenko (1986).

3. Dual distorted profiles

Examples of ambiguous solutions were considered for the first time by Afanas'ev, Aleksandrov, Fanchenko, Chaplanov & Yakimov (1986), who showed that, in the case of crystals without surface relaxation, the two sets of atomic plane Debye–Waller factors e^{-W_n} and $e^{-\tilde{W}_n}$, related by

$$e^{-\tilde{W}_n} = 1 - e^{-W_{N-n+1}}, \tag{5}$$

produced the same rocking curves.

For the analysis of similar examples, it is convenient to define the new variables c_n,

$$\begin{aligned} c_1 &= \exp(-W_1 + i\varphi_1), \\ c_{N+1} &= 1 - \exp(-W_N + i\varphi_N), \\ c_n &= \exp(-W_n + i\varphi_n) - \exp(-W_{n-1} + i\varphi_{n-1}) \\ & \qquad n = 2, \ldots, N, \end{aligned} \tag{6}$$

satisfying the apparent identity

$$\sum_{n=1}^{N+1} c_n = 1. \tag{7}$$

It is also convenient to define the relative intensity $\tilde{I}(\Delta\theta) = I(\Delta\theta)/I_0(\Delta\theta)$ expressed in terms of the new variables as

$$\tilde{I}(\Delta\theta) = \left| \sum_{n=1}^{N+1} c_n \exp(iqn) \right|^2. \tag{8}$$

As is seen from (8), if a set of numbers c_n is the solution of the problem under consideration, the set

$$\tilde{c}_n = c^*_{N-n+2} \tag{9}$$

is also a solution and gives the same diffraction intensity. This transformation applied to the scattering characteristics gives

$$\exp(-\tilde{W}_n + i\tilde{\varphi}_n) = 1 - \exp(-W_{N-n+1} - i\varphi_{N-n+1}), \tag{9*}$$

this relation being a generalization of (5).

It is natural to name the solutions $\{\exp(-W_n + i\varphi_n)\}$, $\{\exp(-\tilde{W}_n + i\tilde{\varphi}_n)\}$ related as in (9*) the dual solutions. The initial solution $\{\exp(-W_n + i\varphi_n)\}$ should satisfy the condition

$$\exp(-W_n) \le 1. \tag{10}$$

In general, the dual solution $\{\exp(-\tilde{W}_n + i\tilde{\varphi}_n)\}$ with new $\exp(-\tilde{W}_n)$ values may violate the condition

$$\exp(-\tilde{W}_n) \le 1. \tag{10*}$$

If (10*) is violated for some n, the dual solution should be eliminated as a non-physical one. The different results are accessible in the different cases. For the dual solution $\{\exp(-\tilde{W}_n + i\tilde{\varphi}_n)\}$ to be physical the initial solution should satisfy the inequality

$$\exp(-W_n) \le 2\cos\varphi_n,$$

which is always satisfied in the case of weak subsurface relaxation. The solution transformation (9) is easily generalized on the continuous model with functions $\exp[-W(X) + i\varphi(X)]$ depending on the distorted layer depth X:

$$\begin{aligned} &\exp[-\tilde{W}(X) + i\tilde{\varphi}(X)] \\ &\qquad = 1 - \exp[-W(L-X) - i\varphi(L-X)], \end{aligned} \tag{11}$$

where L is the total distorted layer depth.

In the continuous crystal model it is natural to treat only the functions $\exp(-W + i\varphi)$ satisfying the boundary conditions

$$\begin{aligned} &\exp[-W(0)] = 0, \qquad \exp[-W(L)] = 1, \\ &\varphi(L) = 0. \end{aligned} \tag{12}$$

The function class considered above is invariant under dual transformation (9), *i.e.* the dual solution satisfies the boundary conditions (12) if the initial solution satisfies them. The transformation (11) may be rewritten in a more symmetrical form:

$$\begin{aligned} &\exp[-W(X)] \\ &\qquad = \sin\tilde{\varphi}(L-X)/\sin[\tilde{\varphi}(L-X) + \varphi(X)] \\ &\exp[-\tilde{W}(X)] \\ &\qquad = \sin\varphi(L-X)/\sin[\varphi(L-X) + \tilde{\varphi}(X)]. \end{aligned} \tag{13}$$

As is apparent from the new dual-solution representation (13), the corresponding Debye–Waller factors are equal for $\varphi(X) \equiv \tilde{\varphi}(X)$, the solution being a self-dual one, *i.e.* invariant under the dual transformation. Physical self-dual solutions are obtained from (13) with the function $\varphi(X) \equiv \tilde{\varphi}(X)$ satisfying the conditions

$$\begin{aligned} 0 \le \varphi(X) &\le \pi/2 \\ 0 \le \varphi(X) + \varphi(L-X) &\le \pi/2. \end{aligned}$$

The dual-solution different examples are illustrated in Figs. 3 and 4. The phase and Debye-Waller curves I, $\tilde{\text{I}}$ represent solutions with different monotonicity properties. Curves II, $\tilde{\text{II}}$ represent the dual solutions with equivalent monotonicity properties, the monotonic growth condition being insufficient for the unambiguity. Curve III represents a solution with an unphysical dual partner, curve IV represents a self-dual solution.

4. General analysis

As is clear from (8) for the relative intensity, $\tilde{I}(\Delta\theta) \equiv 1$ for an ideal crystal. $\tilde{I}(\Delta\tilde{\theta})$ differs in practice from 1 for some $\Delta\tilde{\theta}$, the number of essentially distorted subsurface atomic planes N being given by

$$N \simeq \tan\theta_B / 4\Delta\tilde{\theta}.$$

Let us now consider a quantitive analysis which gives the possibility of the reconstruction of the coefficients c_n and of the corresponding $\exp(-W_n + i\varphi_n)$ from the experimentally obtained relative intensity function $\tilde{I}(\Delta\theta)$. In fact, we consider the reconstruction of all diffraction amplitudes leading to the same intensity. The real part of the amplitude may be reconstructed for $q \to 0$ directly from (2*) and (3), but this information is insufficient for reconstruction of all the $\exp(-W_n + i\varphi_n)$.

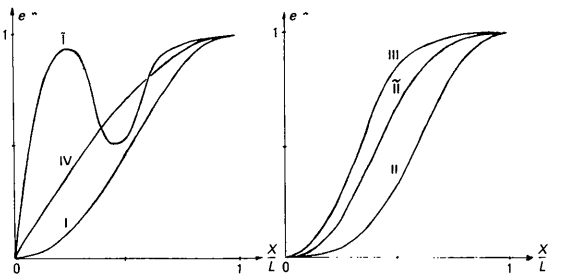

Fig. 3. Debye-Waller factors of the dual distorted profiles. Curves I, $\tilde{\text{I}}$ and II, $\tilde{\text{II}}$ represent the solutions interconnected by the dual transformation. Curve III represents the profile with an unphysical dual partner. Curve IV represents a self-dual profile.

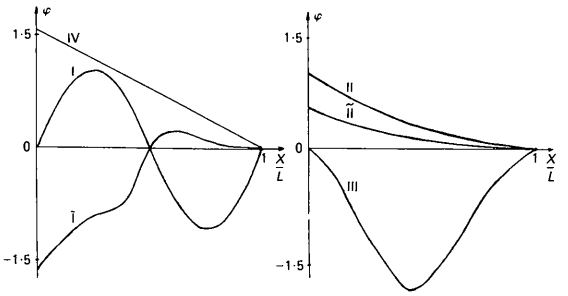

Fig. 4. Phases of the dual distorted profiles. Curve notations are the same as those in Fig. 3.

To solve the ambiguity problem one should consider (8) and assume that some distorted profile with phases φ_n^0, Debye-Waller factors $\exp(-W_n^0)$ and corresponding coefficients c_n^0, given by (6), is known. Introducing the notation $z = e^{iq}$ and the polynomial

$$P_N(c, z) = \sum_{n=1}^{N+1} c_n z^{n-1}, \tag{14}$$

we may express the relative intensity $\tilde{I}(\Delta\theta)$ as

$$\tilde{I}(\Delta\theta) = (1/z^N) P_N(c^0, z) P_N(\tilde{c}^0, z),$$

where $\tilde{c}^0$ is related to c^0 in dual transformation (9). Our aim is to obtain all the sets of coefficients c_n leading to the same $\tilde{I}(\Delta\theta)$ and consequently to the same polynomial,

$$F_{2N}(c^0, z) = P_N(c, z) P_N(\tilde{c}, z). \tag{15}$$

If z_n represents the roots of the polynomial $P_N(c^0, z)$, then $1/z_n^*$ will be the roots of the polynomial $P_N(\tilde{c}^0, z)$, all these roots being simultaneously the roots of the polynomial $F_{2N}(c^0, z)$. One may pick out in a new way the N roots of the new polynomial $P_N(c, z)$ from the given $2N$ roots of the polynomial $F_{2N}(c^0, z)$, the remaining roots being the roots of the new polynomial $P_N(\tilde{c}, z)$. One may take z_n or $1/z_n^*$ as the nth root of the polynomial $P_N(c, z)$; hence the total number of possible sets of roots of the polynomial $P_N(c, z)$ and of the corresponding sets c_n is 2^N, the coefficients of the polynomial $P_N(c, z)$ being unambiguously related to its roots. With the normalization condition (7) one may express coefficients c_N *via* the roots $t_1, \ldots, t_N$ of $P_N(c, z)$ in the following way:

$$\begin{aligned} c_{N+1} &= \prod_{n=1}^{N} 1/(1 - t_n) \\ c_{N+1-n} &= (-1)^n c_{N+1} \sum_{1 \le i_1 < \ldots < i_n \le N} \prod_{m=1}^{n} t_{i_m} \qquad n = 1, \ldots, N. \end{aligned} \tag{16}$$

Substituting all roots z_n of $P_N(c^0, z)$ by $1/z_n^*$, we reproduce the dual transformation (9) discussed above. In general there exist 2^N different solutions c_n leading to the same diffraction intensity. One should pick out only the physical solutions which satisfy the condition (10). Their number may be large or small in different cases.

Re $M_N(0)$ is invariant under the root transformation $z_n \to 1/z_n^*$ discussed above. One should note that this transformation produces no new solution for $|z_n| = 1$, hence the number of different solutions is essentially decreased when the absolute value of some roots is equal to unity. The degenerate cases are accessible as the absolute values of all roots are equal to unity and the reconstruction problem is then unambiguous.

Let us consider an example of the complete self-conjugated solution with the distorted profile

$$e^{-W_n} = n/(N+1) \qquad n = 1, \ldots, N$$
$$\varphi_n = 0. \tag{17}$$

The corresponding polynomial roots are given by the expression

$$z_n = \exp[i2\pi n/(N+1)] \qquad n = 1, \ldots, N.$$

The transformations discussed above do not change the original profile (17), but small distortions of this profile lead to destruction of the degeneracy and to the ambiguity.

The above analysis is naturally simplified in the case of the large layer number $N \gg 1$. One should divide the distorted layer into sublayers consisting of k monolayers and consider e^{-W} and Δd to be constant for each sublayer. If the inequalities

$$k\Delta\theta \ll \tan\theta_B \quad \text{and} \quad k\Delta d \ll d_0$$

and the condition (4) are satisfied, the sublayer diffraction amplitude is equivalent to the monolayer diffraction amplitude M_N, equation (1), with the value $\Delta\theta$ substituted by $k\Delta\theta$. The monolayer-scattering-characteristics reconstruction analysis is therefore valid for the sublayer analysis as well. The spatial resolution in the sublayer case is k times decreased compared with the monolayer one because the diffraction data are considered only for the region of deviation angle $\Delta\theta$ being k times less than the monolayer one. As a rather large number of different sets $\exp(-W_n + i\varphi_n)$ leading to the same diffraction intensity exists, it is convenient to vary the roots S_n of the corresponding multinomial $P_N(c, z)$ instead of the parameters $\exp(-W_n)$, φ_n in the experimental rocking-curve analysis, the total number of parameters being invariant. The relative intensity is the following function of the complex parameters S_n:

$$\tilde{I}(\Delta\theta) = \prod_{n=1}^{N} |(e^{iq} - S_n)/(1 - S_n)|^2.$$

This expression is invariant under the transformations $S_n \to 1/S_n^*$ in agreement with the previous analysis, hence these parameters S_n may be reconstructed from the known function $\tilde{I}(\Delta\theta)$ in the polycircle $|S_n| \le 1$, this problem being unambiguously solved by variational methods. After reconstruction of the N roots in the polycircle $|S_n| \le 1$, one should check all 2^N sets of roots of polynomial $P_N(c, z)$ that contain S_n or $1/S_n^*$ as the nth root, and reconstruct from (16) the corresponding c_n and all the sets with physical scattering characteristics of the distorted layer. Examples of experimental data analysis based on the above method have been considered recently by Zav'alova, Imamov, Lomov, Marguschev & Maslov (1987).

5. Bicrystal diffraction analogues

In order to demonstrate the abilities of the method under consideration it is convenient to consider the simplest distorted profile with e^{-W} and Δd constant and to find its equivalents analytically. The polynomial $P_N(c^0, z)$ is represented in this case as

$$P_N(c^0, z, e^{-W}) = [(1-z)\,e^{-i\alpha N} + z^N(e^{-W} - 1) + z^{N+1}(1 - e^{-W+i\alpha})]/(z - e^{-i\alpha}), \qquad \alpha = 2\pi\Delta d/d_0. \tag{18}$$

Considering firstly the case without partial amorphization, *i.e.* with $e^{-W} = 1$, one can reduce (18) as follows:

$$P_N(c^0, z) = \frac{e^{-i\alpha N} + z^{N+1}(1 - e^{i\alpha}) - z\,e^{-i\alpha N}}{(z - e^{-i\alpha})}.$$

It is easy to show that all the roots of the equation $P_N(c^0, z_k) = 0$ satisfy the condition

$$(\sin|\alpha|/2)^{1/N} < 1/|z_k| < \tfrac{1}{2} + (\tfrac{1}{4} + 2\sin|\alpha|/2)^{1/2}.$$

The last expression shows that all the root magnitudes tend to unity for large N and small α; hence the perturbation theory in the small parameter $1 - |z_k|$ is available. Introducing the notation $z_k = r_k \exp(i\psi_k \operatorname{sign}\alpha)$, one can obtain the following equations for ψ_k, r_k $(1 - r_k \ll \sin\psi_k/2)$:

$$\psi_k = 2\pi(2k-1)/(2N+1) - |\alpha| + 2(1 - r_k)/|\alpha|(2N+1)r_k^{N+1/2} + \pi(1 \mp 1), \tag{19}$$
$$\psi_k \in [0, 2\pi), \qquad r_k^{N+1/2}\sin|\alpha|/2 = \sin\psi_k/2,$$

with α of order of magnitude $1/N$ and all values of order $1/N^2$ being neglected.

If the root numbers k satisfy the inequality

$$|2\pi(2k-1)/2N + 1 - |\alpha|| \le 1/N$$

then equations (19) reduce to the following equations for $\rho_k = (N + \frac{1}{2})(r_k - 1)$:

$$|\alpha|\,e^{2\rho_k} \pm [|\alpha| - 2\pi(2k-1)/(2N+1)]\,e^{\rho_k} \pm \rho_k/|\alpha|(N+\tfrac{1}{2})^2 = 0$$

with the signs $\pm$ corresponding to the signs in (19).

If the root numbers k satisfy the inequality

$$|2\pi(2k-1)/(2N+1) - |\alpha|| \ge 1/N \tag{20}$$

then (19) may easily be simplified and the following solution is obtained for ψ_k, r_k:

$$\psi_k = 2\pi(2k-1)/(2N+1) - |\alpha| + 2\pi\theta[|\alpha| - 2\pi(2k-1)/(2N+1)],$$
$$\theta(X) = \begin{cases} 1 & X > 0 \\ 0 & X \le 0 \end{cases}$$
$$r_k = [\sin(\psi_k/2)/\sin(|\alpha|/2)]^{1/(N+1/2)}. \tag{21}$$

Assuming inequality (20) to be satisfied for all N roots in the following analysis, one may use expressions (21) for all roots. As is shown in the Appendix, the Debye-Waller factors may be directly expressed *via* the corresponding roots of the polynomial $P_N(c, z)$. Considering the root set, differing from the initial one in p root transpositions $z_n \to 1/z_n^*$, one may express the corresponding Debye-Waller factors in the following way within the above approximation:

$$\exp(-W_n) = 1 + 2\sum_k^p \frac{1-r_k}{\sin[\pi(2k-1)/(2N+1)]} \times \sin\frac{\pi(2k-1)(2n-1)}{2N+1}, \qquad (22)$$

with the sum being taken over all p transpositions. For the analysis of (22) one should consider the dependence of r_k on α. It is apparent from (21) that all $r_k > 1$ in the case of $|\alpha| < \pi/(2N+1)$. It can be shown exactly, and is also seen from (21), that $r_1 = 1$ for $\alpha = \pi/(2N+1)$. One may also easily show that the first k root magnitudes are less than unity for $|\alpha| \in [\pi(2k-1)/(2N+1), \pi(2k+1)/(2N+1))$. Hence, by increasing α one tends to decrease r_k and, correspondingly, the physical-solution number.

Indeed, it can be seen from (22) that the Debye-Waller-factor corrections increase as the r_k decrease.

In order to show that the bicrystal has no physical analogues for $\varphi = N\alpha > \pi/(2+1/N)$, let us firstly consider the case of one root transposition. As is seen from (22), the transposition of the first root, with absolute value r_1 being less than unity for $\varphi > \pi N/(2N+1)$, gives $\exp(-W_1) > 1$. Although the sign of $1 - r_k$ is arbitrary in the case of the kth root transposition, one can always find two distorted-atomic-plane numbers, m_1, m_2, that satisfy the inequalities

$$\sin\frac{\pi(2k-1)(2m_1-1)}{2N+1} > 0,$$

$$\sin\frac{\pi(2k-1)(2m_2-1)}{2N+1} < 0,$$

and result in the Debye-Waller factor $\exp(-W_{m_1})$ or $\exp(-W_{m_2})$ being greater than unity in this case.

The situation is analogous in the case of the transpositions of the two roots. Indeed, the previous analysis is valid for transpositions of the first and kth roots, and in the case of transposition of k_1th and k_2th roots, $k_1, k_2 \neq 1$, one can always find two numbers m_1, m_2, that satisfying the inequalities

$$\sin\frac{\pi(2k_1-1)(2m_1-1)}{2N+1} > 0$$

$$\sin\frac{\pi(2k_2-1)(2m_1-1)}{2N+1} > 0$$

$$\sin\frac{\pi(2k_1-1)(2m_2-1)}{2N+1} < 0$$

$$\sin\frac{\pi(2k_2-1)(2m_2-1)}{2N+1} < 0.$$

These inequalities result in an unphysical m_1th or m_2th Debye-Waller factor. It is natural to assume that this situation will be the same for the larger number of root transpositions with expression (22) containing a sum of a large number of terms with large phases and the transposition-sum sign being distinct for different n. Hence, one can conclude that the bicrystal has no physical analogues in the case of sufficiently large phases. This approximate analytical analysis has been justified by the exact numerical calculations carried out for $N \leq 12$, and the absence of the bicrystal physical analogues has been confirmed in the case of $|\varphi| > \pi N/(2N+1)$ (the numerical calculations for sufficiently larger N are time consuming).

However, the situation is essentially different in the case of the bicrystal with $e^{-W} < 1$. Instead of (22), one can easily obtain the following expression for the Debye-Waller factors reconstructed from the root sets with the p root transpositions executed:

$$\exp(-W_n) = \exp(-W)\left\{1 + 2\sum_k^p \left[\frac{1-\tilde{r}_k}{\sin(\alpha+\tilde{\psi}_k)/2} \times \sin\frac{\alpha+\tilde{\psi}_k}{2}(2n-1)\right]\right\}, \qquad (23)$$

$$\tilde{z}_k = \tilde{r}_k \exp(i\tilde{\psi}_k),$$

where $\tilde{z}_k$ are the polynomial roots of (18). The derivation of (23) is given in the Appendix.

The difference between z_k and $\tilde{z}_k$ may be neglected in the case of $1 - e^{-W} \ll 1$; hence, one can use (21) for the roots within the above approximation. The magnitudes of the roots with numbers satisfying the inequality

$$k \leq [|\alpha|(2N+1)/2\pi] + \tfrac{1}{2}$$

are less than unity, and the value of e^{-W_1} obtained by the p transpositions of these roots may be evaluated as

$$e^{-W_1} = e^{-W}(1 + 2p|\alpha|).$$

Hence, these transpositions result only in the unphysical solutions in the case of $|\alpha| > (1 - e^{-W})/2$. Let us consider the contribution to the Debye-Waller factor value e^{-W_n} of the other root transpositions with root magnitudes greater than unity.

As is easily seen from (21), all the root magnitudes tend to unity with the growth of $|\alpha|$, thus decreasing the corrections to the initial Debye-Waller factors. With the sum of a large number of sines with large phases being of the order of unity and not of the order of the term number it is easy to show that if

the rather weak condition

$$e^{-W} \lesssim 1-(1/N)\ln(2N/|\varphi|) \qquad (24)$$

is satisfied, the transpositions of the roots with magnitudes greater than unity lead to some new physical solutions. Hence, the number of the bicrystal physical equivalents N_F may be evaluated as

$$N_F \simeq 2^{(N-1/2-|\varphi|/\pi)}. \qquad (25)$$

The greater the phases $|\varphi|$ the better is inequality (24) satisfied. Hence, as is seen from (25), the tendency of the physical solution number to decrease is rather weak and the problem under consideration may become an unambiguous one only in the case of $\Delta d \sim d_0$. Thus, there exists a rather large number of bicrystal physical analogues even for relatively small Debye-Waller-factor deviations from 1.

In the case of $N=10$, $\varphi=\pi$, $e^{-W}=0{\cdot}8$, exact numerical calculations were carried out and 375 bicrystal physical analogues were discovered. Our previous qualitative analysis predicts ~500 bicrystal analogues, in rather good agreement with the numerical calculations.

One should note that the partial crystal amorphization is always present in the cases of the ion implantation; hence, the many-solution interpretation of the rocking curves is necessary at least in this problem. The large number of physical analogues of the bicrystal with $e^{-W}<1$ demonstrates the complexity of the reconstruction of the distorted profiles from the diffraction intensity data for the relatively large distorted layer number. The numerical calculation analysis shows that one can hardly analyse the above problem for $N_{\max} \geq 20$ with reasonable computer time; besides, the large number of rather similar solutions of our problem makes the usual direct variational fit of the parameters e^{-W} and Δd fruitless. Hence, it is not possible to arrive at a much better spatial resolution than

$$L_{\min} = (\tan\theta_B) d_0 / 4\Delta\theta_{\max} N_{\max},$$

where $\Delta\theta_{\max}$ is the maximum angular deviation from the Bragg angle in the experiment.

For an unambiguous profile reconstruction some additional information is needed. One can use the scattering-phase data obtained from the secondary-processes data, and mainly from the electron photoemission data (Afanas'ev, Aleksandrov & Imamov, 1986). This additional information may sufficiently decrease the number of possible solutions of the reconstruction problem. The above problem of the reconstruction of all the equivalent diffraction-amplitude Fourier-component sets is a rather general one and is similar to the phase problem in optics and to the problems of low-energy electron diffraction (LEED). Hence, the above methods may be useful for these problems as well.

APPENDIX

It is convenient to use Cauchy's theorem for reconstruction of the phase and Debye-Waller factors from the roots of the polynomial $P_N(c, z)$:

$$\exp(-W_m + i\varphi_m) = (1/2\pi i)\oint_{r_0} [P_N(c,z) - z^N]\, dz/z^m(1-z) \qquad m = 1, \ldots, N \quad (26)$$

where r_0 is a closed contour in the vicinity of the origin. The integrands in (26) may be multiplied by an arbitrary analytical function $f(z)$ with the following asymptotic behaviour at $z \to 0$:

$$f(z) = 1 + O(z^N).$$

Choosing the following expression for $f(z)$,

$$f(z) = 1/(1-z^N),$$

and taking into consideration the fact that the integrands deductions at infinity

$$\operatorname{res}[P_N(c,z) - z^N] f(z)/z^m(1-z)$$

are equal to zero, one can express the integral *via* the sum of the deductions in the $f(z)$ poles and obtain the following expression for $\exp(-W_m + i\varphi_m)$ that can easily be found by the inverse discrete Fourier transformation and is useful in the case of small roots t_k:

$$\exp(-W_m + i\varphi_m) = \frac{1}{N}\sum_{n=1}^{N} \frac{t_n}{t_n - 1} + \frac{1}{N}\sum_{n=1}^{N-1} \left\{ \left[\prod_{l=1}^{N} \frac{\exp(i2\pi n/N) - t_l}{1-t_l} - 1 \right] \times \frac{\exp[-i2\pi n(m-1)/N]}{1-\exp(i2\pi n/N)} \right\}. \qquad (27)$$

The simple sum rule is obtained from (27):

$$\sum_{m=1}^{N} \exp(-W_m + i\varphi_m) = \sum_{m=1}^{N} t_m/(t_m - 1).$$

However, it is convenient to choose the following function $f(z)$ in the bicrystal case:

$$f(z) = (1-z)/(z - e^{-i\alpha}) P_N(c^0, z, e^{-W}),$$

where $P_N(c^0, z, e^{-W})$ is given by (18).

Multiplying the integrand in (26) by $f(z)$, one can reduce (26) to

$$\exp(-W_m + i\varphi_m) = \frac{1}{2\pi i}\oint_{r_0} \frac{dz}{z^m} \prod_{k=1}^{N} \frac{z - t_k}{(1-t_k)(z - \tilde{z}_k)} \times \frac{\exp(-i\alpha N)}{[z - \exp(-i\alpha)][1 - \exp(-W + i\alpha)]}, \qquad (28)$$

where the root set t_n differs from the polynomial (18) root set $\tilde{z}_n$ in the p root transpositions $\tilde{z}_k \to 1/\tilde{z}_k^* = t_k$. By deforming the integration contour in (28) one may express all the $\exp(-W_m + i\varphi_m)$ as the sums of $(p+1)$ deductions in the integrand poles, the deduction at infinity being equal to zero, and obtain the result

$$\exp(-W_m + i\varphi_m)$$

$$= \exp[-W + i\alpha(m - N - 1)]$$

$$\times \prod_k^p \frac{(1-\tilde{z}_k)[1 - z_k^* \exp(-i\alpha)]}{(1-\tilde{z}_k^*)[\exp(-i\alpha) - \tilde{z}_k]}$$

$$\times \left[1 - \sum_k^p \frac{\exp(-im\alpha)}{\tilde{z}_k^m} \frac{|\tilde{z}_k|^2 - 1}{\tilde{z}_k^* \exp(-i\alpha) - 1}\right.$$

$$\left. \times \prod_{l \neq k}^p \frac{\exp(-i\alpha) - \tilde{z}_l}{\exp(-i\alpha) - 1/\tilde{z}_l^*} \frac{\tilde{z}_k - 1/\tilde{z}_l^*}{\tilde{z}_k - \tilde{z}_l}\right],$$

where all the sums and products are taken over all the transpositions executed.

As all the bicrystal root magnitudes $|\tilde{z}_k|$ tend to 1, the following expression for Debye-Waller factors may be obtained to first order in $1 - |\tilde{z}_k|$:

$$\exp(-W_m) = \exp(-W)\left\{1 + 2\,\mathrm{Re}\sum_k^p \left[\frac{\exp(-im\alpha)}{\tilde{z}_k^m} \times \frac{1 - |\tilde{z}_k|}{\tilde{z}_k^* \exp(-i\alpha) - 1}\right]\right\}.$$

References

AFANAS'EV, A. M., ALEKSANDROV, P. A., FANCHENKO, S. S., CHAPLANOV, V. A. & YAKIMOV, S. S. (1986). *Acta Cryst.* A**42**, 116-122.

AFANAS'EV, A. M., ALEKSANDROV, P. A. & IMAMOV, R. M. (1986). *Rentgenovskay Structurnay Diagnostica v Issledovanii Pripoverchnostnich Sloyev Monocrystallov.* Moscow: Nauka.

AFANAS'EV, A. M., ALEKSANDROV, P. A., IMAMOV, R. M., LOMOV, A. A. & ZAV'ALOVA, A. A. (1984). *Acta Cryst.* A**40**, 352-355.

AFANAS'EV, A. M. & FANCHENKO, S. S. (1986). *Dokl. Akad. Nauk SSSR*, **287**, 1395-1399.

AFANAS'EV, A. M., KOVALCHUCK, M. V., KOVEV, E. K. & KOHN, V. F. (1977). *Phys. Status Solidi A*, **42**, 415-420.

AFANAS'EV, A. M., KOVALCHUCK, M. V., LOBANOVICH, E. F., IMAMOV, R. M., ALEKSANDROV, P. A. & MELKONYAN, M. K. (1981). *Sov. Phys. Crystallogr.* **26**, 13-20.

AWANO, H., SPERIOSU, V. S. & WILTS, C. H. (1984). *J. Appl. Phys.* **55**, 3043-3048.

BONSE, V., HART, M. & SCHWUTTKE, G. H. (1969). *Phys. Status. Solidi*, **33**, 361-366.

BURGEAT, J. & COLELLA, R. (1969). *J. Appl. Phys.* **40**, 3505-3509.

BURGEAT, J. & TAUPIN, D. (1967). *Acta Cryst.* A**24**, 99-103.

EISENBERGER, A. M., ALEXANDROPOULOS, N. G. & PLATZMAN, P. M. (1972). *Phys. Rev. Lett.* **28**, 1519-1525.

HALLIWELL, M. A. G., LYONS, M. H. & HILL, M. J. (1984). *J. Cryst. Growth*, **68**, 523-531.

KAMENOU, K., HIRAI, I., ASAMA, K. & SAKAI, M. (1979). *J. Appl. Phys.* **34**, 539-542.

QUILLEC, M., GOLDSTEIN, L., LE ROUX, G., BURGEAT, J. & PRIMOT, J. (1984). *J. Appl. Phys.* **55**, 2904-2909.

SPERIOSU, V. S., GLASS, H. L. & KOBAYASHI, T. (1979). *Appl. Phys. Lett.* **34**, 539-542.

TAKAGI, S. (1962). *Acta Cryst.* **15**, 1311-1316.

TAUPIN, D. (1964). *Bull. Soc. Fr. Minéral. Crystallogr.* **87**, 469-475.

YAKIMOV, S. S., CHAPLANOV, V. A., AFANAS'EV, A. M., ALEKSANDROV, P. A., IMAMOV, R. M. & LOMOV, A. A. (1984). *Pis'ma Zh. Eksp. Teor. Fiz.* **39**, 3-5.

YOGI, K., MIYAMOTO, N. & NISHIZAVA, J. (1970). *J. Appl. Phys.* **9**, 246-250.

ZAV'ALOVA, A. A., IMAMOV, R. M., LOMOV, A. A., MARGUSCHEV, Z. C. & MASLOV, A. V. (1987). *Krystallografiya.* In the press.

Acta Cryst. (1988). A**44**, 33-37

The Statistical Significance of Difference Densities

BY E. N. MASLEN

Crystallography Centre, University of Western Australia, Nedlands 6009, *Western Australia*

(*Received* 31 *March* 1987; *accepted* 11 *August* 1987)

Abstract

The statistical properties of a difference density $\Delta\rho$ are not fully characterized by the standard deviation $\sigma(\Delta\rho)$, which relates to the density at a point. That is not sufficient information to assess the significance accurately for the density within a finite volume. The reliability of a complete $\Delta\rho$ map may be determined by applying standard statistical tests to the chi-square index

$$\chi^2 = \sum_{\mathbf{s}} \sigma^{-2}(\mathbf{s})[\Delta F(\mathbf{s})]^2$$

from a least-squares refinement, where ΔF is a structure-factor residual and σ^2 is the variance in the structure factor, or equivalently to the goodness-of-fit

0108-7673/88/010033-05$03.00